Isothermal Oxidation of TiAl Alloy

R.G. REDDY, X. WEN, and M. DIVAKAR

Isothermal oxidation behavior of Ti-48.6 at. pct Al alloy was studied in pure dry oxygen over the temperature range 850 °C to 1000 °C. The oxidation was essentially parabolic at all temperatures with significant increase in the rate at 1000 °C. Effective activation energy of 404 kJ/mol was deduced. The oxidation products were a mixture of TiO_2 (rutile) and α-Al_2O_3 at all temperatures. An external protective layer of alumina was not observed on this alloy at any of the temperatures studied. A layered structure of oxides was formed on the alloy at 1000 °C.

I. INTRODUCTION

TITANIUM aluminides offer improved performance compared to the conventional high-temperature materials such as superalloys owing to their low density and good creep resistance.[1–4] However, the oxidation characteristics of titanium aluminides at high temperatures are a major concern. In general, unlike Ni-Al alloys, a protective Al_2O_3 layer does not form on all the Ti-Al alloys because both Ti and Al form oxides of very similar stability. Aluminum forms a very slow growing oxide (α-Al_2O_3), while titanium forms several oxides (TiO, TiO_2, Ti_2O_3, *etc.*), which have relatively high growth rates. It has been observed that a protective continuous layer of alumina is formed on Ti-Al alloys containing more than the stoichiometric amount of Al. $TiAl_3$ is the only compound on which a protective, continuous α-Al_2O_3 was found to exist over a wide temperature range. [5–8] A nonprotective TiO_2(rutile) phase was found to be the major oxide constituent on the surface of Ti_3Al at elevated temperatures.[9,10] In the case of a TiAl stoichiometric compound, Ti-rich scales were formed at elevated temperatures resulting in an increase in the parabolic rate constant[9] by several orders of magnitude. Meier *et al.*[11] studied the oxidation behavior of TiAl in air and oxygen and have observed that TiAl does not form a protective layer of α-Al_2O_3 but forms scales composed of TiO_2 and Al_2O_3. Their results indicate that the alloys in the Al-rich portion of the TiAl field formed a protective layer over the temperature range 1100 °C to 1300 °C.

In this study, isothermal oxidation of Ti-48.6 at. pct Al alloy was studied in pure dry oxygen over the temperature range of 850 °C to 1000 °C. Oxidation rate constants were obtained from the weight gain curves using the parabolic law. The oxidation product was a mixture of TiO_2 and Al_2O_3 at all the temperatures of measurement. The rate of oxidation was rapid at 1000 °C and the scale spalled midway through the oxidation.

II. EXPERIMENTAL PROCEDURE

The alloy samples were prepared by arc melting 99.9 pct pure Ti wires and 99.9 pct pure Al rods in a copper hearth under the flow of purified argon using the tungsten electrodes. The ingots containing 51.4 at. pct Ti and 48.6 at. pct Al (numbers henceforth refer to atom percent in the paper) were homogenized at 1000 °C for 18 hours in argon atmosphere and later cut into experimental samples of approximately 10-mm-diameter and 1-mm-thick discs using a low speed diamond saw. The samples were polished using 600 grit emery papers and ultrasonically cleaned in acetone. The oxidation kinetics of samples was studied by weight gain measurements using a thermogravimetric (TGA) setup detailed elsewhere.[12] The sample was suspended in a Lindberg furnace by a platinum wire whose top end is attached to the Cahn Model electrobalance. The temperature of the furnace was varied from 850 °C to 1000 °C. A continuous supply of pure dry oxygen was maintained throughout the experiment at each temperature. The weight change of the sample was measured by the electrobalance whose output was recorded continuously by an X-Y recorder. The oxide morphologies were examined by a PHILIPS* XL30 scanning electron microscope (SEM) with energy-dispersive x-ray analysis (EDX). The composition of the oxidized region was estimated by a PHILIPS Xpert X-ray Diffractometer.

*PHILIPS is a trademark of Philips Electronic Instruments Corp., Mahwah, NJ.

III. RESULT AND DISCUSSION

A. *Oxidation Kinetics*

Figure 1 shows the weight gained per unit surface area of the alloy samples oxidized in pure dry oxygen as a function of time at different temperatures. The oxidation data obtained from the literature[11] are also plotted in the figure for the sake of comparison. The oxidation rate was found to increase with temperature. In comparison with the literature data,[11] the rate of oxidation was found to decrease with aluminum content of the alloy. At 850 °C and 950 °C, the oxidation kinetics was parabolic. However, at 1000 °C, the oxidation rate increased significantly and the kinetics changed from parabolic to linear after about 140 minutes of oxidation. Hence, the oxidation data at 1000 °C up to 140 minutes was used in the analysis of the oxidation kinetics and the data was fit to the parabolic rate equation as follows:

$$\left(\frac{\Delta W}{S}\right)^2 = k_p t \qquad [1]$$

R.G. REDDY, ACIPCO Professor, X. WEN, Graduate Student, and M. DIVAKAR, Postdoctoral Research Fellow, are with the Department of Metallurgical and Materials Engineering, The University of Alabama, Tuscaloosa, AL 35487-0202.

Manuscript submitted November 7, 2000.

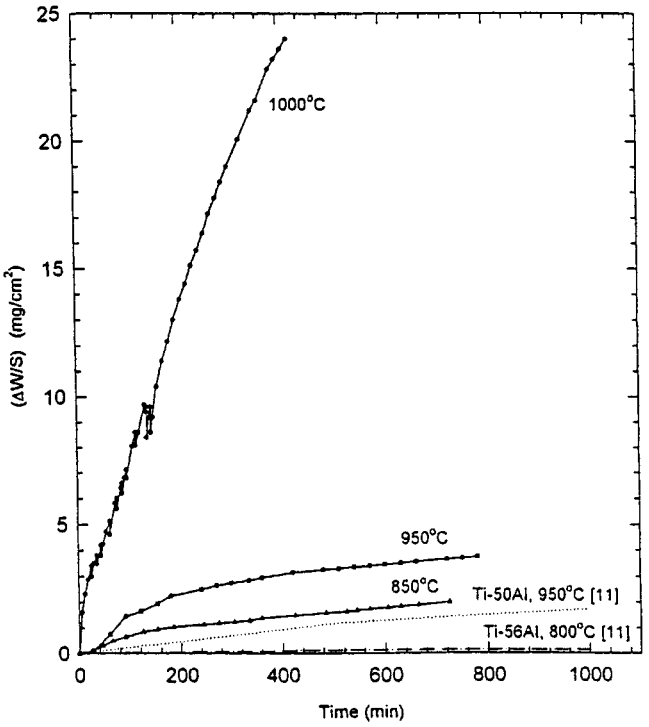

Fig. 1—Weight gain *vs* time for Ti-48.6Al alloy oxidized at different temperatures in pure dry oxygen.

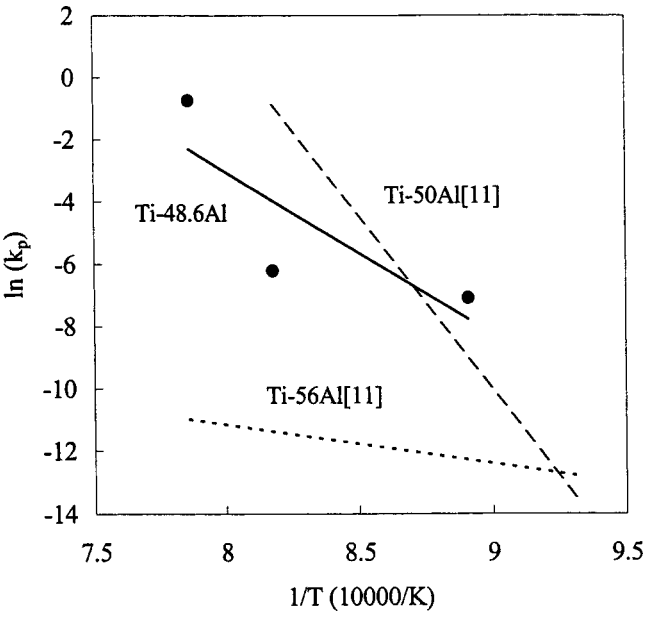

Fig. 2—In (k_p) *vs* 1/*T* for Ti-48.6Al oxidized in pure dry oxygen.

where ($\Delta W/S$) is the weight gain per unit surface area of the specimen, k_p is the parabolic rate constant, and t is the oxidation time. The temperature dependence of k_p can be expressed by

$$k_p = k_o\, e^{(Q/RT)} \qquad [2]$$

where k_o is a constant and Q is the effective activation energy for the oxidation. Taking the natural logarithm on both sides yields

Table I. Activation Energies of Oxidation for Ti-Al Alloys

Alloy	Reference	Q_{eff}, kJ/mol
Oxidation of Ti	13	235
Oxidation of Ti-26Al	10	255
Oxidation of Ti-32Al	9	299
Oxidation of Ti-34Al	10	299
Oxidation of Ti-48.6Al	this work	404
Oxidation of Ti-49Al	10	419

Table II. Phases Identified by X-ray Diffraction in the Oxidized Scale of Ti-48.6Al Alloy

850 °C	950 °C	1000 °C
TiO	TiO	TiO_2
TiO_2	TiO_2	Ti_2O_3
α-Al_2O_3	α-Al_2O_3	α-Al_2O_3

$$\ln (k_p) = \ln (k_o) - \frac{Q}{RT} \qquad [3]$$

Figure 2 shows the plot of ln (k_p) *vs* 1/*T* for the TiAl alloy oxidized in pure dry oxygen. Linear regression of the plot yields an effective activation energy Q of 404 kJ/mol for oxidation. Table I shows the effective activation energies for the oxidation of Ti and TiAl binary alloys obtained from the literature[9,10,13] along with that of the present alloy. It can be seen that the activation energy increases with the aluminum concentration of the alloy, suggesting that the oxidation mechanism was different in alloys containing higher aluminum contents.

B. *Oxide Scale Composition and Morphology*

Table II shows the phases present in the oxidized scale on the Ti-48.6Al alloy at different temperatures. The oxide scale comprised of a mixture of TiO_2 and Al_2O_3. No ternary phases such as Al_2TiO_5 were found in the scale at any of the temperatures in this study. These results are in agreement with the observations made by Becker *et al.*[14] The thermodynamic aspects of the oxidation of stoichiometric TiAl alloy have been well discussed by Rahmel and Spencer in their article.[15] They estimated the phase diagram of Al_2O_3-TiO_2 based on the thermodynamic calculations and have shown that the ternary oxide, Al_2TiO_5 is stable above 1010 °C. Our results are in concurrence with their prediction.

The thermodynamic stability of the base metal oxide (TiO_2) in the Ti-Al based alloys is similar to that of Al_2O_3. The thermodynamics and kinetics of the oxidation of Ti-48Al alloy were reviewed by Kekare and Aswath,[16] where they presented a model to represent the mechanism of oxidation in air. Although there are small differences in the mechanisms of oxidation in air and in pure oxygen owing to the presence of nitrogen in air, the stages of oxidation proposed by them concur well with our observations in this study. Becker *et al.*[14] have discussed the mechanism of isothermal oxidation of Ti-Al alloys in pure oxygen and air. Oxidation of any metal proceeds by two processes, oxygen dissolution and oxide scale formation. During the initial stages of oxidation, molecular oxygen from the gas phase is adsorbed on the alloy surface and dissociates. A layer of continuous oxide

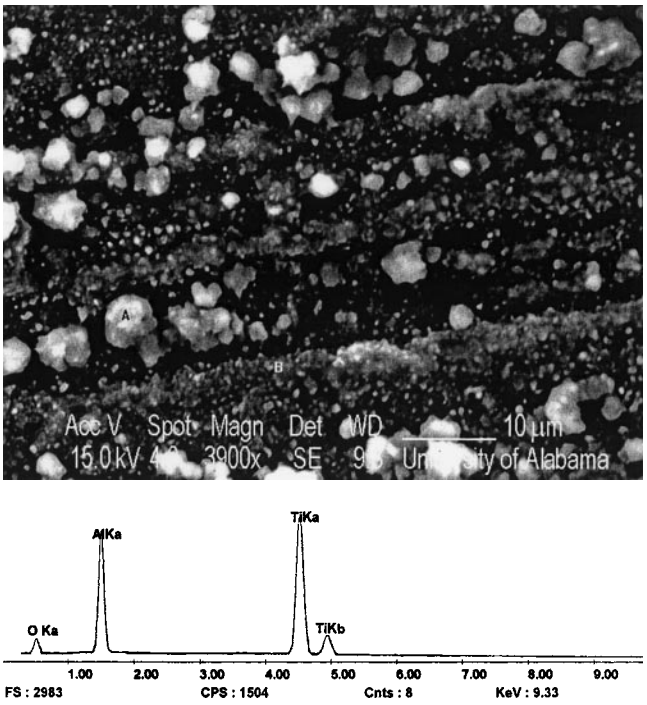

Fig. 3—SEM micrograph and EDX spectrum showing the morphology of the oxidized surface of Ti-48.6Al alloy oxidized at 850 °C for 24 h in pure oxygen. Nuclei of (*a*) TiO_2 and (*b*) Al_2O_3 are seen in the micrograph.

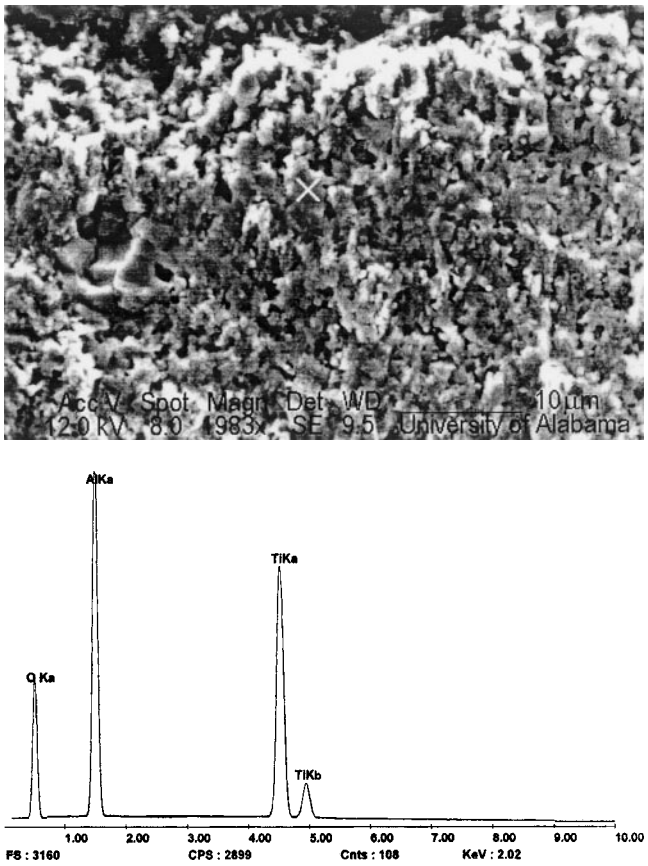

Fig. 4—SEM micrograph showing the morphology of the oxide scale of Ti-48.6Al alloy oxidized at 950 °C for 24 h in pure oxygen. An EDX spectrum of the region marked (x) is also shown.

film is formed by the nucleation and lateral growth of oxide crystallites. Thus, the oxidation process includes the initial surface reaction, which is thermodynamically controlled, followed by growth of oxide film, which is determined predominantly by the rate of diffusion of oxygen ions through the oxide scale and alloy surface.

Besides, α-Al_2O_3, titanium forms a series of oxides (TiO, TiO_2, Ti_2O_3, *etc.*) whose thermodynamic stabilities are similar to that of alumina. However, the thermodynamic analysis can be used to determine only the initial surface reaction and the phase stability. The initial oxidation product is determined by the relative stability of several oxides that could form depending on the temperature, activities of Al and Ti in the alloy, and the partial pressure of oxygen at the oxygen/metal interface. Subsequently, the growth of oxide is determined by the rates of diffusion of Ti, Al, and O ions through the oxide scale. Since the diffusivity of Ti in TiO_2 (rutile) is faster than that of oxygen, and Al diffuses at a very slow rate in alumina, the oxidation of the Ti-Al alloy results in an outward growth of TiO_2 (rutile) and an inward growth of alumina.

Figure 3 shows the SEM micrograph and EDX spectrum of the sample oxidized at 850 °C. Oxide nuclei of both TiO_2 and Al_2O_3 are formed at preferred nucleation sites on the surface of the alloy. An inhomogeneous mixture of tiny TiO_2 and Al_2O_3 crystallites could be seen in the micrograph. This indicates that, besides the inward diffusion of oxygen, the outward diffusion of Ti and Al ions also plays an important role in the formation of the crystals. However, when the oxide scale becomes thick, the growth rate is controlled by the diffusion of oxygen vacancies since the diffusion of Ti and Al ions through the oxides is much slower compared to that of oxygen ions.

Figure 4 shows the SEM micrograph and EDX spectrum of the Ti-48.6Al alloy oxidized at 950 °C for 24 hours. The oxide nuclei that formed at 850 °C (Figure 3) grew to form an oxide network comprised of TiO_2 and Al_2O_3. The EDX spectrum of the region marked by (×) shows the presence of both the oxides. The oxide scale mostly consisted of a mixture of Al_2O_3 and TiO_2 with small amounts of TiO. They are distributed inhomogeneously in the scale with the outer layer enriched in TiO_2.

At 1000 °C, a layered structure comprised of TiO_2 and Al_2O_3 is formed. Figures 5(a) to (d) show the morphologies of the oxides formed at 1000 °C along with the EDX spectra obtained at various regions of the micrographs.

Although TiO_2 and Al_2O_3 have similar thermodynamic stability, TiO_2 grows faster than Al_2O_3. It is known that TiO_2 (rutile) has a tetragonal configuration with columns of filled octahedral sites along the *c*-axis direction, and a similar parallel column of empty octahedral sites, which provides a faster diffusion path for the transport of oxygen ions. Thus, TiO_2 nuclei grow faster and form a pure TiO_2 outermost layer followed by an intermediate layer consisting of both TiO_2 and Al_2O_3 and finally a layer enriched in α-Al_2O_3. These layers are formed depending on the partial pressure of oxygen present at the oxide/alloy interface and the activities of Ti and Al in the alloy adjacent to the interface.

Figure 5(a) shows large crystals of pure TiO_2 formed in the outermost layers of the oxide scale. A densely packed α-Al_2O_3 layer having a crystal size smaller than TiO_2 is formed beneath the outer layer, as can be seen from the markers in Figure 5(b). Figure 5(c) shows another SEM

micrograph indicating the different orientations of the oxide scale with different compositions marked as 1, 2, and 3. The EDX spectrum of region 2 in Figure 5(c) indicates that the oxide scale consists of both TiO_2 and Al_2O_3 but is enriched in Al_2O_3. Figure 5(d) is a backscattered micrograph of the fractured cross section, which shows a layered structure formed at 1000 °C. The EDX spectrum corresponds to the upper region (marker 1) of the oxide scale that is predominantly TiO_2 with a small amount of Al_2O_3. Adjacent to the alloy surface (between markers 1 and 2), a thick region containing a mixture of Al_2O_3 and TiO_2 was found. It appears that this area might have been formed as a result of the

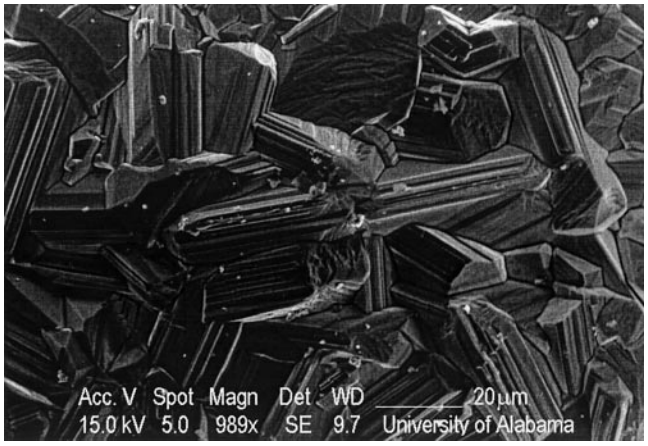

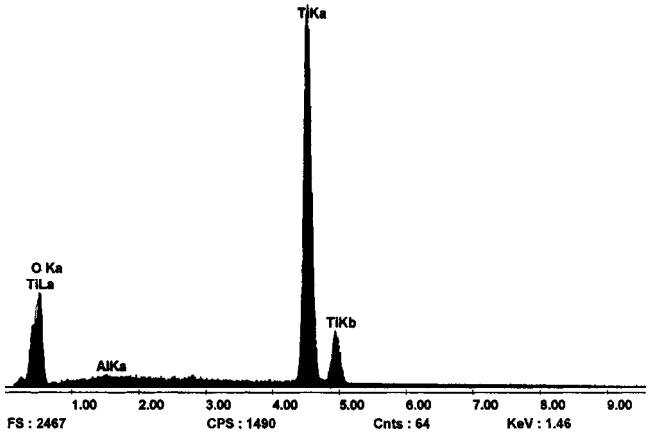

(*a*)

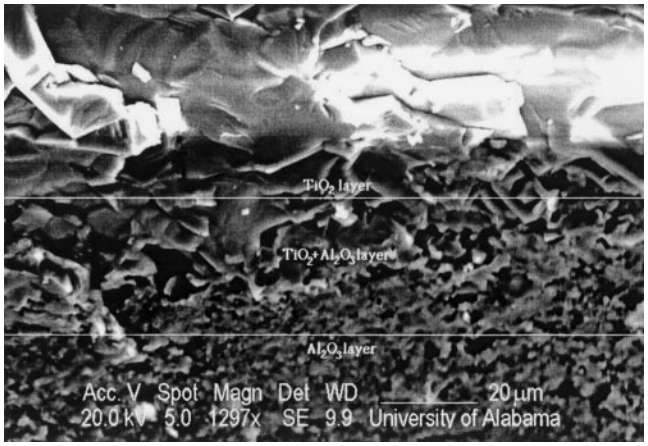

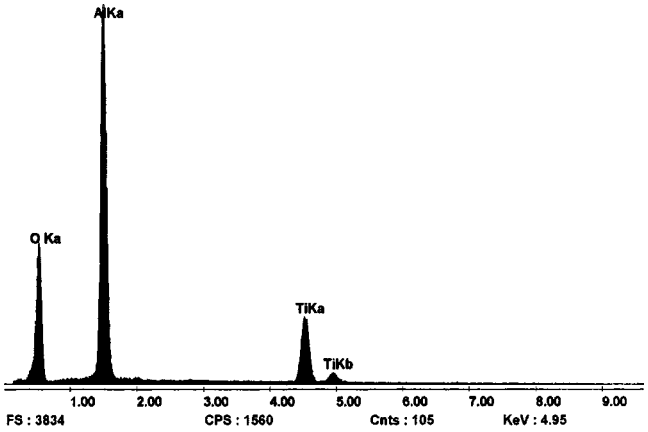

(*b*)

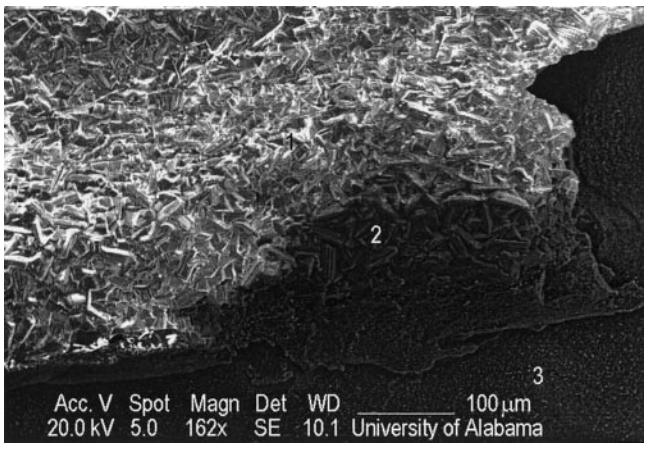

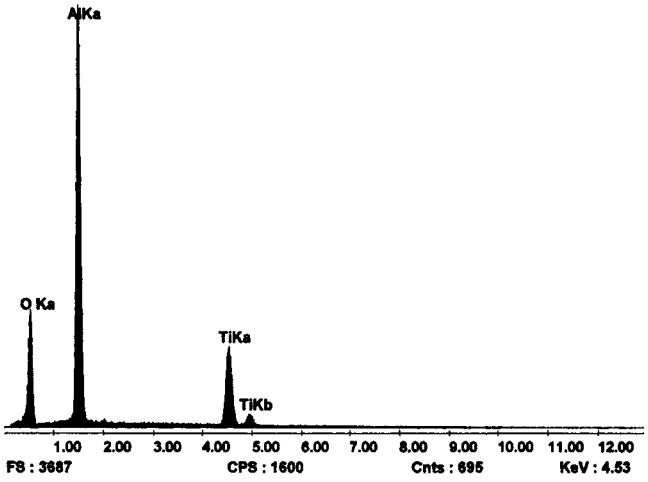

(*c*)

Fig. 5—SEM (*a*) micrograph and EDX spectrum showing large crystals of TiO_2 on the outer layer of the Ti-48.6Al alloy oxidized at 1000 °C for 24 h in pure oxygen. (*b*) SEM micrograph and EDX spectrum showing small crystals of Al_2O_3 beneath the TiO_2 outer layer of the Ti-48.6Al alloy oxidized at 1000 °C for 24 h in pure oxygen. (*c*) SEM micrograph showing the different orientations of the oxide scale of Ti-48.6Al alloy oxidized at 1000 °C, 24 h in pure oxygen. Compositions of regions: (1) Al_2O_3, (2) Al_2O_3 + TiO_2, and (3) TiO_2. An EDX spectrum of region (2) is also shown.

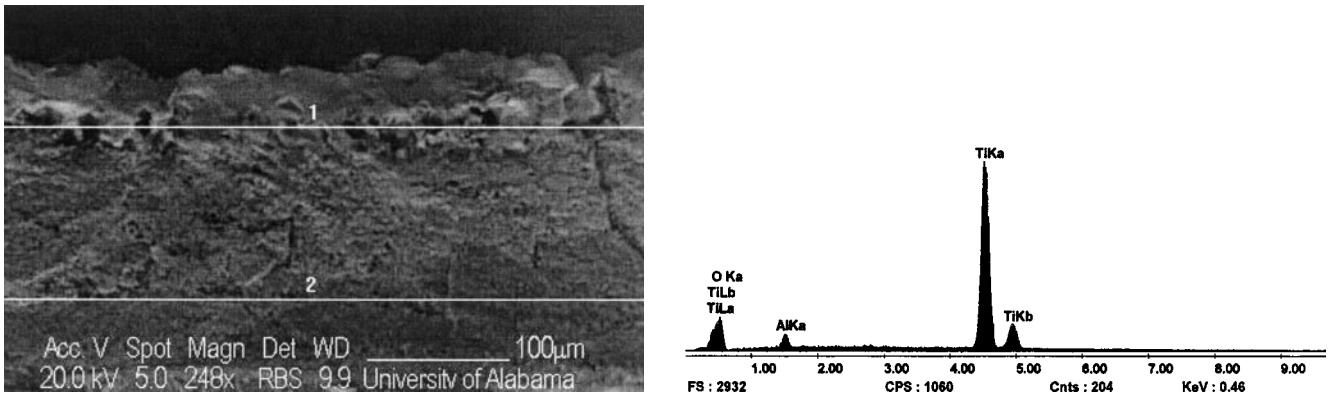

(*d*)

Fig. 5—Continued. (*d*) Backscattered SEM micrograph showing the fractured cross section through the oxide scale of the Ti-48.6Al alloy oxidized at 1000 °C for 24 h in pure oxygen. An EDX spectrum of the upper region (marker 1) of the oxide layer is also shown.

sintering of several sublayers.[10] The overall oxide layer is about 200-μm thick. Many voids could be seen across the entire thickness of the oxidized scale. The upper portion of the alloy surface beneath the outer oxide layer (marker 1) underwent internal oxidation and displayed internal cracking because of oxygen embrittlement.

As the oxide grows, the thermal mismatch stresses along with the orientation strains between the alloy and oxide phases result in breakaway of the oxide layer. Fast outward diffusion of Ti leaves behind a small amount of porosity at the TiO_2/α-Al_2O_3 layer boundary. These voids increase the alloy oxidation rate by providing paths for rapid diffusion within the oxide scale resulting in embrittlement of the scale.

IV. CONCLUSIONS

1. The oxidation kinetics of the Ti-48.6Al alloy obey the parabolic law in the temperature range of 850 °C to 1000 °C.
2. At 1000 °C, the oxidation rate was rapid and the kinetics changed from parabolic to linear after about 140 minutes of oxidation.
3. The activation energy of 404 kJ/mol for oxidation of the Ti-48.6Al alloy was deduced.
4. The oxidation scale on the TiAl alloy mainly contains a mixture TiO_2 and Al_2O_3. No ternary oxides were found at any of the temperatures in this study.
5. A layered structure with alternate layers of TiO_2 and Al_2O_3 was formed at 1000 °C. The results obtained in this study concur well with earlier observations on the system.

ACKNOWLEDGMENTS

The authors are pleased to acknowledge the financial support from the National Science Foundation, Grant No. DMR-9696112.

REFERENCES

1. S.G. Kumar and R.G. Reddy: *Metall. Mater. Trans. A*, 1996, vol. 27A, pp. 1121-26.
2. S.G. Kumar, R.G. Reddy, J. Wu, and J. Holthus: *J. Mater. Eng. Perf.*, 1995, vol. 4 (1), pp. 63-69.
3. S.G. Kumar, R.G. Reddy, and L. Brewer: *J. Phase Equil.*, 1994, vol. 15 (3), pp. 279-84.
4. S.G. Kumar and R.G. Reddy: *Proc. Int. Symp. on Synthesis/Processing of Lightweight Metallic Materials*, TMS, Warrendale, PA, 1995, pp. 129-39.
5. N. Birks, G.H. Meier, and F.S. Pettit: *JOM*, 1994, vol. 46, pp. 42-46.
6. J. Subrahmanyam: *J. Mater. Sci.*, 1989, vol. 23, pp. 1906-10.
7. J.L. Smialek: *Corr. Sci.*, 1993, vol. 35 (5–8), pp. 1199-1208.
8. R.G. Reddy and X. Wen: *EPD Congr. '97*, TMS, Warrendale, PA, 1997, pp. 47-54.
9. X. Wen and R.G. Reddy: *Processing and Fabrication of Advanced Materials*, TMS, Warrendale, PA, 1996, pp. 379-89.
10. G. Welsch and A.I. Kahveci: in *Oxidation of High-Temperature Intermetallics*, T. Grobstein and J. Doychak, eds., TMS, Cleveland, OH, 1998, pp. 207-18.
11. G.H. Meier, D. Appalonia, R.A. Perkins, and K.T. Chiang: *Oxidation of High-Temperature Intermetallics*, T. Grobstein and J. Doychak, eds., TMS, Cleveland, OH, 1988, pp. 185-93.
12. R.G. Reddy and R.B. Inturi: *Min. Metall. Processing*, 1999, vol. 16 (20), pp. 46-50.
13. J. Unnam, R.N. Shenoy, and R.K. Clark: *Oxid. Met.*, 1986, vol. 26, pp. 231-52.
14. S. Becker, A. Rahmel, M. Schorr, and M. Schütze: *Oxid. Met.*, 1992, vol. 38 (5–6), pp. 425-64.
15. A. Rahmel and P.J. Spencer: *Oxid. Met.*, 1991, vol. 35, pp. 53-68.
16. S.A. Kekare and P.B. Aswath: *J. Mater. Sci.*, 1997, vol. 32 (9), pp. 2485-99.